Locomotion of Miniature Catom Chains: Scale Effects on Gait and Velocity

David Johan Christensen
Maersk Mc-Kinney Moller Institute
University of Southern Denmark
Odense, Denmark

david@mip.sdu.dk

Jason Campbell
Intel Research Pittsburgh
Pittsburgh, Pennsylvania, USA

jason.d.campbell@intel.com

Abstract—Scaling down the module size of a self-reconfigurable robot will have a profound effect on the module's characteristics, e.g. strength to mass ratio. In this paper we explore how the characteristics of chains of modules, specifically locomotion velocity and best gait type, might change with the scale of those modules. The simulated experiments we report on here examine module sizes from ($11\mu m$ to $698\mu m$ radius) and chain lengths from 3 to 30 modules. All gaits tested were based on central pattern generators optimized using a genetic algorithm and hill climbing. Our results show that scaling affects both the preferred type of gait as well as a chain's overall performance (average velocity). In summary, there is a tradeoff where larger scales face the challenge of overcoming gravity, while smaller sizes face the challenge of staying in contact with the ground and the friction it provides. We show that in between these two extremes lies a "best" module size for given environmental, physical, and engineering constraints.

I. Introduction

Self-reconfigurable robots consist of interconnected robotic modules that can autonomously change the way that they are interconnected. Self-reconfiguration between different configurations allows such robots to adapt their morphology to address the requirements of diverse situations. One example would be changing configuration from a walker to a snake to traverse a narrow passage.

State-of-the-art self-reconfigurable robots consist of up to a few dozen centimeter-scale modules. Increasing the number of modules in a given robot increases the flexibility with which the ensemble can adapt — much as complex biological systems are composed of more parts (cells) than simpler ones. Thus we are concerned with scaling up the number of modules (to billions) while scaling down the size of the individual modules (to microns). This paper considers the latter case of scaling down the size of the module, while varying the number of modules in the range from 3 to 30. Our approach does not scale directly to larger groups of modules. However, much as biological systems use the same basic structures (e.g. cilia or muscle fibers) repeatedly, we envision that small chains of modules can be used as basic building blocks that can be assembled into more complex robots.

This paper addresses what we will loosely term "snake-like" locomotion of chains of miniature spherical modules (as shown in Figure 1). The ability of small ensembles to locomote is important in a number of situations: A self-assembly scenario could involve modules that are initially separated, but which move in small groups to cluster together and form a connected mass. Another example is moving
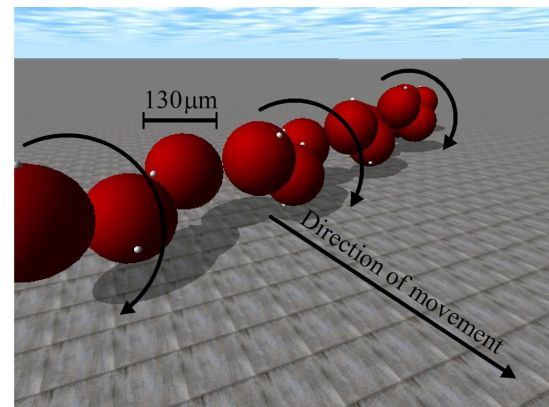

Fig. 1. An illustration of the fastest gait found amongst 25 different module sizes and 15 different chain lengths. It was optimized using a genetic algorithm followed by hill-climbing. The gait is a spiraling motion, similar to the sidewinding of snakes, and its average velocity is $0.11m/s$. The chain contains 14 modules and the module radius is $65\mu m$.

through tiny cracks or holes exploring a pile of rubble for survivors after an earthquake. A third example would be tiny, swimming modular robots that could find an application in non-invasive micro-surgery.

To explore scale effects on locomotion we define a simple model of a robot module (see Section III-B) based on the modules envisioned by the Claytronics project [3]. The model assumes spherical modules covered with electrostatic surface actuators, and from this we can calculate the maximum torque that one module can exert on another. Three parameters: radius, mass and maximum torque describe the scale dependent characteristics of our modules. Gaits are controlled using central pattern generators (CPGs), which are the artificial equivalent of self-organizing oscillating neurons (see Section IV-C). Two CPGs run on each module to generate the sinusoidal trajectories for steering the yaw and pitch angles between a module and its neighbor. Section IV-D describes the six parameters which defines the gait of a chain. By running a physics simulation (see Section V-A), gait parameters are optimized for speed of locomotion using a combination of hill climbing and a genetic algorithm (described in Section V-C). The simulations enable us to study the effects of scaling — specifically how the velocity and type of gait depend on the module size and chain length (Section VI).
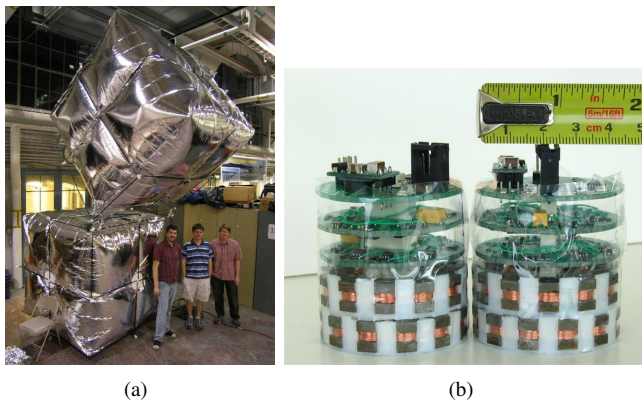
Fig. 2. Two scales of catom modules: (a) Giant helium-filed catoms 1.8 m across, using electrostatic actuation. (b) Cylindrical catoms 44 mm across, using electromagnetic actuation.
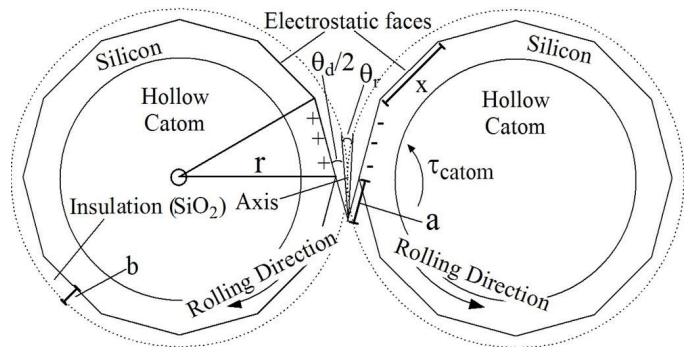

Fig. 3. The electrostatic catom model we use for our analyses assumes insulated plates positioned near the surfaces of spherical modules. When charged, the plates generate a torque around the point of contact.

II. RELATED WORK

The concept of self-reconfigurable robots was first proposed by Fukuda et al. in the late 1980's [2]. Locomotion of self-reconfigurable modular robots has since then been studied on a number of different platforms, including MTRAN [9], PolyPod [14], PolyBot [15], CONRO [1], SuperBot [10] and ATRON [8].

In related work, efficient and effective locomotion has been demonstrated for many different combinations of gaits, configurations, and platforms. Role based [13], hormone based [11] and phase automata patterns [16] are some of the control strategies used to make self-reconfigurable robots move. Genetically optimized central pattern generators (CPG) were used to control MTRAN walkers and snakes [6] [5]. Similarly, CPGs controlling the YaMoR modular robot were genetically evolved and online optimized [7] in order to achieve locomotion.

These approaches are similar to the approach of this paper. They define the interactions between modules and the periodic trajectories to be followed by the module actuators. Further, the approaches allows gaits to be optimized by adjusting parameters such as frequency, phase shift from module to module, amplitude of trajectory, etc.

This work differentiates itself from the above in that the purpose is not to optimize the gaits and configurations for robots assembled from modules with fixed characteristics. Instead, the characteristics of the modules are varied for a fixed type of configuration (chain) to study the effects of scaling down module size.

III. CATOM MODULES

Catom modules serve as a platform for the exploration of the concept of programmable matter [3]. The long term goal of this research effort is to produce physical artifacts that can dynamically change shape and therefore enable applications like, telepresence, interactive 3D design, and smart antennas.

A. Cylindrical Catom Hardware

Current hardware prototypes of catom modules are planar with a cylindrical shape of radius 2.2 cm (see Figure 2(b)). Around the border of the cylinder are 24 electromagnets which can be energized to attract neighboring modules via magnetic forces. This causes one module to spin around another, thereby allowing the group of modules to self-reconfigure and take on a particular shape.

B. Spherical Electrostatic Catom Model

In 3D, catoms are spherical or faceted and can roll across the surfaces of other catoms. Early versions of such catoms have been constructed at the meter scale, using helium filled balloons with electrostatic surfaces for actuation (see Figure 2(a)). Future work is expected to decrease the size to millimeter or micrometer scale using MEMS technology. At such scales the mechanism of actuation is likely to be electrostatics, which motivates us to define a simple electrostatic model of such a module to investigate the potential physical/electrical characteristics of such tiny catoms.

First, we assume a miniaturized catom to be constructed as a 5 micron thick shell of silicon. Insulation, to avoid short circuiting, is assumed to be glass (SiO_2) with a thickness of $b = 1\mu m$. This assumption implies a dielectric breakdown voltage of $200V$. Conservatively we select the voltage drop between the faces to be $V_d = 100V$ for the purpose of our experiments. Second, we assume the spherical surface to be filled with flat square faces (or plates) that can be charged to produce an electrostatic force between adjacent plates on neighboring catoms. The torque around the contact point between two modules will be given by:

$$\tau_{catom} = \frac{x}{2a+x} \frac{\varepsilon_0 \varepsilon_r^2 x}{2(\varepsilon_r \theta_d + \theta_r)^2} \ln(\frac{a+x}{a}) V_\tau^2 \qquad (1)$$

The notation used is shown in Figure 3. Under the given assumptions, for a given scale, there exists an optimum angle between faces and thereby an optimal number of faces, when maximizing the size of the torque. The number of faces increases with the radius. Estimates of the required number of faces on the entire sphere varies from approximately 40

TABLE I

CHARACTERISTICS OF CATOM MODULES AT DIFFERENT SCALES.

Radius (μm)	Catoms lift (#modules against gravity)	Time to rotate (T_{rotate}) (sec. for full rotation)
698	1	0.055
83	5	0.0038
34	10	0.0012
11	25	0.00027

($r = 11\mu m$) to approximately 2300 ($r = 698\mu m$). For each scale we select the optimal number of faces.

Smaller modules would be stronger relative to mass and would therefore be able to move faster. This is due to the increase, when scaling down, in the surface area to volume ratio and thereby torque to mass. Table I summarizes some characteristics of catoms of different sizes. For a given radius, the corresponding number of catoms which one fixed catom can support in a cantilever is shown (i.e., assembled in a stiff horizontal chain, held static against gravity). The time it takes for one catom to be rotated (360 degrees) around another fixed catom in zero gravity is also shown. Notice the large gain in speed and strength when scaling down the module size.

IV. LOCOMOTION OF CATOM CHAINS

A. Defining a Coordinate System for Catom Pairs

In a chain of catoms, each non-terminal catom controls two angles with respect to its two neighbor modules. We assume that the modules are equipped with an accelerometer for measuring the direction of gravity, and furthermore, that modules are able to sense the direction of contact with each of their neighbors, (i.e. the direction vectors pointing from a module's center of mass to its neighbors' centers of mass). The angle in the horizontal plane between the two direction vectors, is defined as the yaw angle of a catom. Similarly, the pitch angle is defined as the angle between the two direction vectors in the vertical plane, aligned with the vector pointing from the center of mass to the contact point. Angle values of $(\theta_{yaw}, \theta_{pitch}) = (0,0)$ correspond to a straight line of catoms. Both angles can be varied within an interval of ± 120 degrees.

B. Controlling the Connection Angles

By charging and discharging the electrostatic faces the catom modules can roll around each other, affecting the yaw and pitch angles between neighbor modules. To control these angles we make the assumption that the modules have a continuous electrostatic surface. This is a reasonable assumption when the number of faces are high. Accordingly, we do not take into consideration the discreteness of the faceted surfaces for purposes of our simulations. Therefore, we can always apply the maximum torque (for a given scale) between any pair of neighboring modules.

An obvious choice for controlling the torque between pairs of modules is a PD or similar type of feedback controller, based on angular error. However, because we want to explore the impact of scaling on modules we desire a single parameterless controller able to handle modules of various sizes equally well. For this reason we use a simple binary control of the torques.

Torques for each of the two angles are considered independently, then combined to a single torque. The direction of the torque for each angle is always towards the desired angle. These two directions (which are orthogonal) are then combined to a single torque axis. That torque corresponds to a pair of forces acting on the surface of two neighbor modules. The directions of these forces are parallel to the line segment joining the centers of the two modules. In the simulation, forces are applied at a fixed distance (10 degrees) from the contact point between the modules. The point of force can then be specified as a angle: $\arctan(\theta_{pitch,error}/\theta_{yaw,error})$ selecting the corresponding quadrant dependent on the sign of the errors. The size of the force, and thereby the torque, is independent on the size of errors and is always the maximum for a given radius.

This controller has been verified to control the selected scales equally well (average angle error) in a simulation of a sinusoid trajectory-following of a 10 module chain in a gravity-free and frictionless scenario.

C. Central Pattern Generator (CPG)

CPGs are special neurons found in vertebrates, able to produce a rhythmic signal without any external sensory input. They are used to control muscles for locomotion. A single artificial CPG will produce a sinusoidal oscillating signal, which can be followed by the actuators of a robot. In this work we adopt the model proposed in [4] and further refined in [7], details are in the cited papers and will not be repeated here. This model is based on two coupled difference equations, describing the angle and velocity of the CPG. Coupling several CPGs of equal frequency together will make them synchronize their signals to a particular phase shift dependent on the coupling strength between them. If there is no loop in the coupling of CPGs, the phase shift from a parent to a child can be set directly. Furthermore, amplitude and frequency can be selected directly for each CPG.

D. Gait Parameters

In the chain, non-terminal modules use two CPG's to control the horizontal and vertical angles (yaw and pitch) between its two neighbor modules. In principle, amplitude, frequency, and a phase offset could be set for each CPG which could be coupled with every other CPG in the robot. However, to reduce the dimensionality of the problem we limit the number of parameters to just six, summarized in Table II.

One parameter is the frequency at witch the CPG oscillates. Frequency it is the only parameter selected in relation to the scale of the modules - this is because smaller modules are relatively stronger and therefore tend to oscillate faster. Frequency is scaled to the characteristic time parameter which is equal to the time it takes for a catom to make one full rotation around another catom in zero gravity. Yaw and pitch amplitude deicide the width and height of the

TABLE II
THE SIX CPG PARAMETERS DEFINING A CHAIN TYPE GAIT.

CPG Gait Parameters	Interval	Explanation
Frequency	$[0.1,2]$	periods per T_{rotate}
Yaw amplitude	$[0,2/3\pi]$	degree of yaw angle
Pitch amplitude	$[0,2/3\pi]$	degree of pitch angle
Yaw phase shift	$[0,\pi]$	between neighbor modules
Pitch phase shift	$[0,\pi]$	between neighbor modules
Pitch to Yaw phase shift	$[0,\pi]$	only at head module

oscillations along the chain of modules. Yaw and pitch phase shift deicide how many periods there are along the length of the module chain. Finally, a sixth parameter sets the phase shift from the pitch CPG to the yaw CPG at the first module of the chain.

CPGs are coupled to synchronize their oscillations with a phase shift. CPGs are coupled as parent to child couplings, from neighbor to neighbor, from chain head to chain tail. Except at the head module, no coupling are made between CPGs controlling the yaw angles and CPGs controlling the pitch angles.

V. EXPERIMENTAL SETUP

A. Physical simulation

Experiments are performed in DPRsim, an Open Dynamic Engine (ODE [12]) based physics simulator designed to simulate claytronics/DPR ensembles. The world consists of a ground surface (coefficients of friction and restitution are 0.7 and 0.3 respectively) and a number of catoms. Each catom is a hollow silicon sphere. Friction between catom modules is infinite, with no slipping when modules rotate around each other. Neighboring modules exert torques upon one another, implemented as a pair of forces acting on the surfaces of the modules. Radius, mass and maximum actuator torque are as predicted by the electrostatic model. The physical simulation includes collisions, gravity and Stoke's drag law (in air). Reynold's number is almost always below 1 in the experiments performed. The simulation runs at a timesteps equal to 1/100 of the time required for a single catom to rotate one full rotation around a stationary catom in zero gravity.

B. Executing a gait

Initially a chain of catoms of a given length and scale lies in a straight line resting on the ground. All CPGs are initialized with the six parameters defining the gait, along with an initial CPG state $(x_0, v_0) = (0, 0.1)$, where x_i decides the angle at timestep i and which avoid a singularity at $(0,0)$. (Note that v in the CPG state vector does not directly correspond to any of the module or chain velocity values.)

Modules are controlled in a distributed fashion. At every time step they exchange neighbor-to-neighbor messages to synchronize their CPGs. Catoms attempt to follow the trajectories generated by the CPGs, by applying forces to the surfaces of neighbor catoms. After a few oscillations the CPGs are synchronized and the gait as described by its parameters are executed by the robot. Not all selected
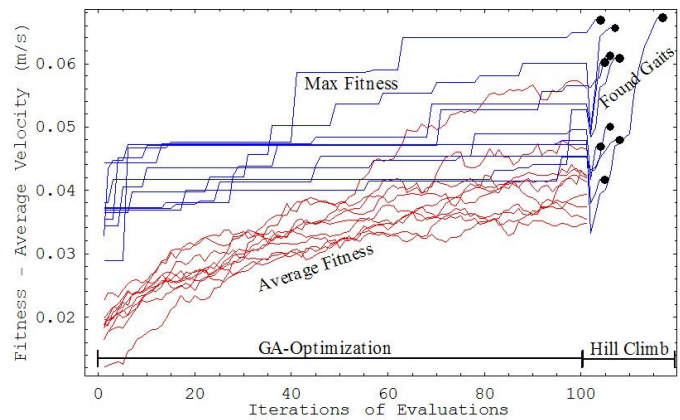

Fig. 4. GA optimization combined with simple hill climbing is used to improve gaits. The example fitness graph here shows ten different runs of gait optimization being performed on a chain of 10 modules with radius $83\mu m$ (able to lift a 5 catom cantilever against gravity). The reevaluation of the best GA discovered gait at the beginning of hill climbing causes the fitness drop around iteration 100.

trajectories can be followed, but we make no attempt to correct this.

C. Finding Gaits: Genetic Algorithm & Hill Climbing

We optimize the velocity of the gaits, by optimizing the six gait parameters via a genetic algorithm. Each gait parameter is encoded as a gene. We use a steady state algorithm with a binary tournament selection of two parents. A single crossover point is randomly chosen. Mutation is performed on the child, with 10% likelihood a random gene will be replaced by a new random value. The child replaces the weaker of two randomly chosen individuals in the population (binary tournament selection). The initial size of the population is 20 random individuals, 100 iterations of child reproduction, replacement and evaluation are performed. An example run is shown in Figure 4.

The fittest individual found in the genetic algorithm is then further optimized using a simple hill-climbing strategy. Small mutations are made to the best-so-far individual until an better individual is found. The process is repeated until there has been no improvement for 25 iterations of mutation and evaluation.

Fitness evaluation of the gaits is based on the horizontal velocity of the chain. We measure a chain's velocity as sum of horizontal distances moved by its center of mass in the duration of 20 CPG periods:

$$fitness = \sum_{i=1}^{20} \frac{P_{cm,i} - P_{cm,i-1}}{20 \cdot Frequency \cdot T_{rotate}} \ (meter/seconds) \quad (2)$$

The smallest-scale modules often make little contact with the ground — due to their high mass/torque ratio most actions send them flying. We want to avoid locomotion gaits which only touch the ground very rarely, since a chain out of contact with the ground is out of control and likely to consume most of its energy lifting. Therefore, we assign zero fitness to gaits which at the time of evaluation are too far from the ground (with "too far" defined as every module more than

Scale Effects on Velocity
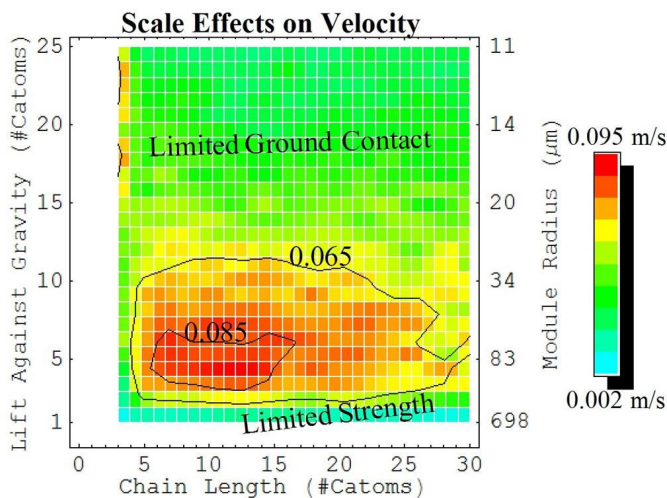

Velocity Variation of Gaits

Fig. 5. Density plot showing the average velocity as a function of chain length and module strength/radius. Each combination of chain length and module size are optimized 10 times using a genetic algorithm and hill climbing. We observe that there exists an area with highest average velocity around 6-16 modules and radius (54μ to $110\mu m$).
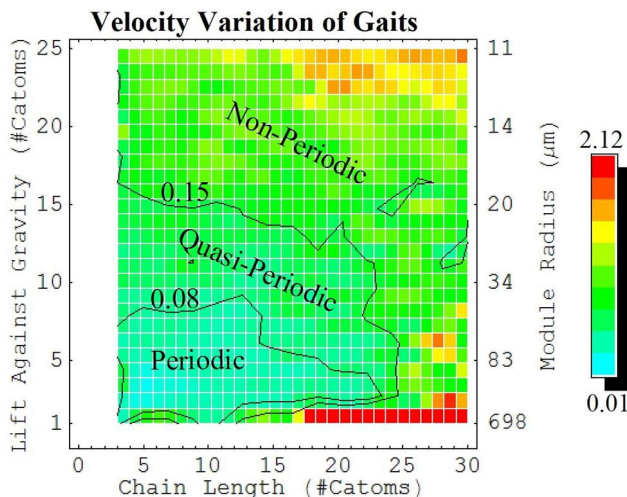
Fig. 6. Density plot showing the average standard deviation of velocity divided by the mean velocity for gaits. This is a measure for how periodic a given gait is. Periodic gaits are more likely for catom sizes corresponding to the area of the fastest gaits.

0.5 radius from the ground). The average gait velocity, used in diagrams, are measured during 200 CPG periods to limit the amount of noise

VI. RESULTS

We performed a total of 3750 gait optimizations using the strategy described above. Experiments were performed for 15 different chain lengths ranging from 3 to 30 modules and for 25 different sizes of module radius varying from $11\mu m$ to $698\mu m$. Module sizes were selected based on the number of catoms that a single catom can lift against gravity when arranged in a horizontal chain. The 25 sizes corresponds to catoms able to lift 1 to 25 other catoms, this selection strategy results in a greater density at the smaller catom sizes. Ten optimizations for average velocity were performed for each combination of length and size. Each optimization yields a single, fastest gait found for that length and size. We then use the characteristics of these gaits to analyze scaling effects on both the types of gaits and on the average velocity.

A. Scaling Effects on Velocity of Locomotion

Velocity of the catom chains were affected by scaling as shown in Figure 5. Larger modules moved relatively slowly, due to their limited force to mass ratio. As modules get smaller, locomotion increases in speed until some critical size around $80\mu m$. Here, the problem of keeping in contact with the ground reduces their performance dramatically. We also observe, that the velocity depends on the length of the chain. Especially around the fastest scale ($80\mu m$), chains in the interval from 6 to 16 modules move faster than longer chains of more than 17 modules. The fastest gaits move with an average velocity of $0.11m/s$.

Another issue is the degree to which gaits are periodic (can maintain their velocity). For a given gait we measure this as the standard deviation of the velocity divided by the
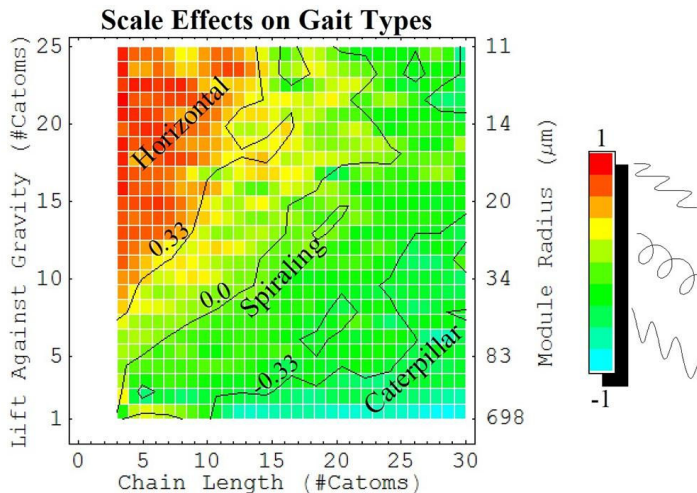
Scale Effects on Gait Types

Fig. 7. Density plot showing the average of a gait-type metric (see text) as a function of chain length and module strength/radius. For larger modules and longer chains the optimizations tend to find gaits with mainly vertical motion (caterpillar). For small catoms and short chains the optimization finds gaits with horizontal motion. In between, predominantly spiraling gaits are found — such gaits are also the fastest seen.

mean velocity (see Figure 6). As can be observed in the diagram only a small fraction of the found gaits are periodic, and these corresponds roughly to the area (size and length) of the fastest gaits. In general, longer chains and smaller modules are less likely to be periodic, due to more complex module-to-module and module-to-environment interactions.

B. Scaling Effects on Types of Gaits

Although the gaits are specified with only six parameters, we have observed a great diversity of gaits, many of which can be recognized as similar to those found in nature. Figure 8 illustrates a few typical example gaits optimized for different scales and for different lengths.

Some typical gaits can be recognized by considering the

(a) Rolling Gait

(b) Spiraling Gait
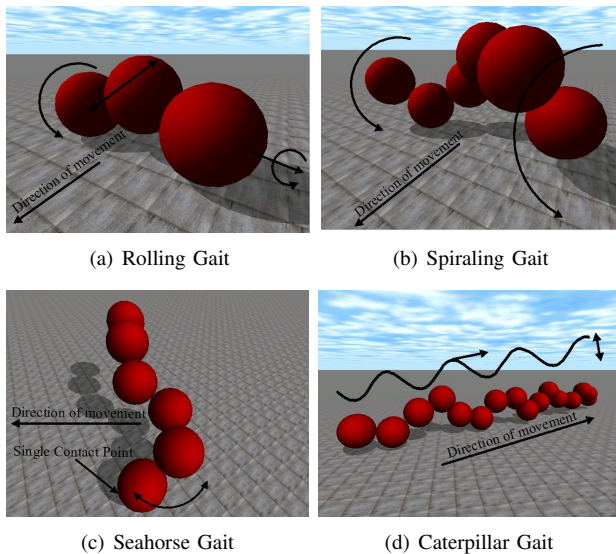

(c) Seahorse Gait

(d) Caterpillar Gait

Fig. 8. Typical gaits at different lengths and scales. Short chains, as (a), often locomote by rolling or hopping. Spiraling gaits, like (b), are typical for medium to long chains of medium size catoms. (c) Seahorse like gaits or pure horizontally oscillating gaits are typical for the smallest catoms. Caterpillar like gaits are typical for large modules and medium to long chains.

normalized difference between the yaw and pitch amplitudes (see Figure 7). Gaits for large modules do generally not have large horizontal movement because of their limited strength. Similar gaits for small modules oscillate only in the horizontal plane to avoid jumping. Gaits for intermediate scales will often be almost perfectly "round" in the sense that they oscillate in both axes strongly, producing a spiral. This spiraling type of gait is somewhat similar to the sidewinding gaits of snakes (see Figure 8(b)). Almost regardless of scale, caterpillar-like gaits seem to be appropriate for longer chains. These produce forward locomotion by having a vertical wave traveling along the length of the chain (see Figure 8(d)).

Alternatively, gaits that can not be recognized from Figure 7 include gaits for short chains which typically hop (in smaller or larger hops) or roll (as in Figure 8(a)), where some of the modules are used as wheels. For the smallest modules most of the gaits found are non-periodic, however, for chain lengths from around 6 to 12 modules there is an alternative strategy. This strategy (see Figure 8(c)) is similar to the movement of seahorses. The modules are aligned in a 45 degree angle to the ground and only a few modules touch the ground. Locomotion is achieved with a relatively slow moment of the tail - pushing on the ground.

C. Parameter Sensitivity

We performed a series of experiments to analyze the gait's sensitivity to changes in the physics/catom models. Using the fastest gait found, a chain consisting of 14 catoms with radius $65\mu m$ (average velocity of $0.11m/s$, see Figure 1), each physics/catom parameter was varied and the impact on maximum velocity (over 50 CPG periods) and rise time (to reach 90% of max velocity) was evaluated. Experiments were

TABLE III

CORRELATIONS BETWEEN PHYSICS/CATOM PARAMETERS AND MAX VELOCITY/RISE TIME

	Interval	Max Velocity	Rise Time
Coeff. of Friction	[0.1, 1.0]	Small (r= .15)	Small (r= 0.11)
Percent of Torque	[0.2, 1.8]	Large (r= .95)	Medium (r= .47)
Coeff. of Restitution	[0.0, 0.9]	Large (r= -.98)	Medium (r= .56)

performed with all except one independent parameter kept fixed while varying the one parameter uniformly across the interval shown in Table III. For each independent parameter approximately 100 experiments were performed.

Table III also shows correlation coefficients that express the strength of the relationship between the parameters. We observe that changing ground friction has almost no effect on the gait in the investigated interval (r= .15). Outside this interval, from friction coefficient 0.1 to 0, max velocity drops very quickly. Torque and max velocity have a strong correlation (r= .95). An increase in the available torque increases the max velocity (from 0.013m/s at 20% to 0.15m/s at 180%) and increases the rise time (from 8 to 17 CPG periods). Also, the coefficient of restitution has a large effect on and a strong correlation (r= -.98) to max velocity. Max velocity is fastest (0.15m/s) and rise time shortest (9 CPG periods) when the coefficient of restitution is 0. For large coefficients of restitution the chain looses contact with the ground and max velocity drops off linearly. For instance, when the coefficient of restitution is 0.9 maximum velocity drops to 0.038 m/s and rise time increase to 31 CPG periods. Finally, we also measured the effect of drag. Drag slows the max velocity of the gait from 0.16m/s (no drag) to 0.12m/s (drag), the difference is statistically significant.

Although both torque and restitution have large influence on max velocity and rise time, these effects occur over relatively large intervals. In conclusion, the gait investigated does not seem to be particularly sensitive to small changes in the physical parameters of the system or the environment.

VII. CONCLUSION & FUTURE WORKS

This paper has experimented with scaling effects on gait and velocity of locomotion for simple chains of catom modules. Scaling in terms of length of chain and size of modules was explored based on a physical simulation of electrostatic catoms. Modules were controlled for locomotion using central pattern generators. Gaits were optimized at varying module sizes ($11\mu m$ to $698\mu m$ radius) and length (3 to 30 modules), using a combination of genetic algorithm and hill climbing.

Our results indicate that very high-velocity gaits 0.11m/s or 1749 module radii per second can result given our assumptions. We observe that there seems to be an appropriate chain length and module size for locomotion - because small modules are uncontrollable since they tend to fly while larger modules are too weak to move. We expect a similar tradeoff to exist for other physical implementations of miniaturized robots and for other tasks such as self-reconfiguration.

Future work will include experimentation with manipulation and locomotion of robots assembled from an increased number of miniaturized catom modules. We envision that the use of structures such as the chains described in this paper can be used as a basic building blocks for assembling robots of increased functionality. The long term goal is to realize robots consisting of billions of miniaturized modules, performing real-life task.

REFERENCES

[1] A. Castano and P. Will. Mechanical design of a module for autonomous reconfigurable robots. In *Proceedings, IEEE/RSJ Int. Conf. on Intelligent Robots and Systems (IROS'00)*, 2000.

[2] T. Fukuda and S. Nakagawa. Dynamically reconfigurable robotic system. In *IEEE Int. Conf. on Robotics & Automation*, 1988.

[3] S. Goldstein, J. Campbell, and T. Mowry. Programmable matter. *Computer*, 38(6):99–101, June 2005.

[4] A.J. Ijspeert. A connectionist central pattern generator for the aquatic and terrestrial gaits of a simulated salamander. *Biological Cybernetics*, 84(5):331–348, 2001.

[5] A. Kamimura, H.Kurokawa, E. Yoshida, S. Murata, K. Tomita, and S. Kokaji. Automatic locomotion design and experiments for a modular robotic system. *IEEE/ASME Transactions on Mechatronics*, 10(3):314–325, June 2005.

[6] A. Kamimura, H. Kurokawa, E. Yoshida, K. Tomita, S. Murata, and S. Kokaji. Automatic locomotion pattern generation for modular robots. In *IEEE International Conference on Robotics and Automation (ICRA)*, pages 714–720, 2003.

[7] D. Marbach and A.J. Ijspeert. Online optimization of modular robot locomotion. In *Proceedings of the IEEE Int. Conference on Mechatronics and Automation (ICMA 2005)*, pages 248–253, 2005.

[8] J. Mikkelsen. Locomotion in ATRON robot systems. Master's thesis, University of Southern Denmark, The Maersk McKinney Moller Institute for Production Technology, July 2005.

[9] S. Murata, A. Kamimura, H. Kurokawa, E.i Yoshida, K. Tomita, and S. Kokaji. Self-reconfigurable robots: Platforms for emerging functionality. In *Lecture Notes in Artificial Intelligence*, volume 3139, pages 312–330. Springer-Verlag, 2004.

[10] W.-M. Shen, M. Krivokon, M. Rubenstein, C. H. Chiu, J. E., and J. B. Venkatesh. Multimode locomotion via superbot reconfigurable robots. *Autonomous Robots*, 20(2):165–177, 2006.

[11] W.-M. Shen, B. Salemi, and P. Will. Hormone-inspired adaptive communication and distributed control for conro self-reconfigurable robots. *IEEE Transactions on Robotics and Automation*, 18:700–712, 2002.

[12] R. Smith. Open dynamics engine. www.ode.org, 2005.

[13] K. Støy, W.-M. Shen, and P. Will. A simple approach to the control of locomotion in self-reconfigurable robots. *Robotics and Autonomous Systems*, 44:191–199, 2003.

[14] M. Yim. New locomotion gaits. In *Proceedings, International Conference on Robotics & Automation (ICRA'94)*, pages 2508 –2514, San Diego, California, USA, 1994.

[15] M. Yim, D.G. Duff, and K.D. Roufas. Polybot: A modular reconfigurable robot. In *Proceedings of IEEE International Conference on Robotics & Automation (ICRA)*, pages 514–520, San Francisco, CA, USA, 2000.

[16] Y. Zhang, M. Yim, C. Eldershaw, D. Duff, and K. Roufas. Phase automata: a programming model of locomotion gaits for scalable chain-type modular robots. In *Proceedings, IEEE/RSJ conference on intelligent robots and systems (IROS)*, Las Vegas, Nevada, USA, 2003.